



Chelating Efficacy and Corrosion Inhibition Capacity of Schiff Base Derived from 3-formylindole

ABY PAUL, K. JOBY THOMAS*, VINOD P. RAPHAEL and K.S. SHAJU

*Associate Professor, Research Division, Department of Chemistry
St. Thomas' College (University of Calicut), Thrissur, Kerala

*Corresponding author E-mail: drjobythomask@gmail.com

(Received: June 20, 2012; Accepted: August 29, 2012)

ABSTRACT

A novel Schiff base derived from 3-formylindole and 2-aminobenzoic acid and its Mn(II), Ni(II) and Cu(II) transition metal complexes were synthesized. Structure of the ligand and complexes were derived on the basis of various analytical techniques such as ¹Hnmr, ¹³Cnmr, infrared, mass and electronic spectroscopy, elemental, magnetic and electrical studies. The corrosion inhibition capacity of the Schiff base on mild steel was screened by Electronic Impedance Spectroscopy (EIS). Investigations showed that the Schiff base act as a good corrosion inhibitor even at low concentrations. The adsorption of inhibitor on the surfaces of mild steel obeys Langmuir isotherm. Thermodynamic parameters (K_{ads} , ΔG°_{ads}) were calculated using Langmuir adsorption isotherm.

Key words: 3-formylindole, 2-amino benzoic acid, transition metal complexes, EIS.

INTRODUCTION

Schiff bases, are organic molecules possessing azomethine linkage (C=N), have innumerable advantages, right from pharmaceutical applications to the corrosion inhibitions, in the various fields of science. Metal complexes of Schiff bases play vital role in the development of coordination chemistry. The studies on coordination compounds of Schiff bases derived from indole carboxaldehydes are seldom reported. But in recent days scientists are more interested in these types of Schiff bases and their metal

complexes¹⁻⁴. The Schiff base complexes derived from 2-aminobenzoic acid are of great importance since they have potential applications in biological systems and chemical fields⁵⁻⁶. In the present course of investigation, a novel potential Schiff base 3-formylindole-2-aminobenzoic acid (3FI2ABA) and its transition metal complexes were synthesized and characterized using various analytical tools and physicochemical studies. The corrosion inhibition capacity of the Schiff base on mild steel in 1M HCl was screened by Electronic Impedance Spectroscopy (EIS).

EXPERIMENTAL

Synthesis of ligand and complexes

1mmol solution of 3-formylindole was dissolved in minimum amount of ethanol (R.S) and boiled. To this hot refluxing solution, equimolar solution of 2-aminobenzoic acid in ethanol was added, refluxed for 2 hours and cooled in ice. The precipitated ligand was filtered, washed with dil. alcohol (1:1) and dried over P₂O₅. 3-formylindole (5mmol) and 2-amino benzoic acid (5mmol) were dissolved separately in ethanol and mixed. It is then refluxed for 2 hours in a hot water bath. To this solution added an alcoholic solution of metal acetate (2.5mmol) and further refluxed for 30 minutes, concentrated by evaporation and cooled in ice. The complex precipitated was filtered, washed with water and dil. alcohol (1:1) and dried over P₂O₅.

Electrochemical Impedance Spectroscopy (EIS)

The EIS measurements of Schiff base were performed in a three electrode assembly. Saturated calomel electrode (SCE) was used as the reference electrode. Platinum electrode having 1cm² area was taken as counter electrode. Mild steel (MS) specimens with an exposed area of 1cm² were used as the working electrode. The EIS experiments were carried out on a Ivium compactstat-e electrochemical system. 1M HCl acid (no deaeration, no stirring) was taken as the electrolyte and the working area of the metal specimens were exposed to the electrolyte for 1 h prior to the measurement. EIS measurements were performed at constant potential (OCP) in the frequency range from 1 KHz to 100 mHz with amplitude of 10 mV as excitation signal. The percentage of inhibitions from impedance measurements were calculated using charge transfer resistance values by the following expression⁷

$$\eta_{EIS} \% = \frac{R_{ct} - R'_{ct}}{R_{ct}} \times 100 \quad \dots(1)$$

where R_{ct} and R'_{ct} are the charge transfer resistances of working electrode with and without inhibitor respectively.

RESULTS AND DISCUSSION

Characterization of the Ligand (3FI2ABA)

The proton magnetic resonance spectrum of the ligand exhibited twelve characteristic peaks due to twelve different types of protons present in the ligand. A peak of singlet nature at 12.14 δ can be assigned to the carboxylic acid proton. Proton of NH moiety present in the indole ring showed its own peak at 6.25 δ as a broad singlet. Signals observed in the range 6.74-8.28 δ are due to aromatic protons of both indole and benzenoid rings. ¹Hnmr data : 12.14 δ , 9.94 δ , 6.52 δ , 6.74-8.28 δ . The proton decoupled ¹³Cnmr spectrum of 3FI2ABA was recorded using DMSO as the solvent and the solvent peak was found at 39.43 δ as septet. The sixteen carbon atoms present in the ligand are of different environment and hence showed their own characteristic signals in the spectrum. As expected, the carboxylate carbon of the Schiff base gave its characteristic signal at 185.57ppm. The azomethine carbon exhibited a sharp peak at 131.71ppm. The non equivalent carbon atoms on both aromatic rings showed their typical peaks between 110-170ppm. ¹³Cnmr data (δ values) : 185.57 δ , 131.71 δ , 110-170 δ .

The molecular ion peak in the mass spectrum of the ligand, 3FI2ABA was appeared at m/z value 264. This gives a good correlation with the molecular weight of the compound. Base peak was recorded at m/z value 219 which may be due to [C₁₅H₁₁N₂]⁺ radical ion. The other significant peaks exhibited in spectrum can be explained by the usual fragmentation pattern of carboxylic acids and imines. A strong band appeared in the infrared spectrum of the ligand at 1570cm⁻¹ can be assigned to stretching frequency of azomethine group. The peaks at 1660cm⁻¹ and 1535cm⁻¹ may be attributed to asymmetric and symmetric stretching frequency of the carboxylate group.

The characteristic bands due to n \rightarrow π^* , $\pi\rightarrow\pi^*$ and n $\rightarrow\pi^*$ transitions are exhibited by the ligand in its electronic spectrum at 26525 cm⁻¹, 28653cm⁻¹ and 40000cm⁻¹ respectively. The spectral studies listed above and the CHN data (C-67.88%, H-4.82%, N-9.75%) suggest the following structure for the ligand 3FI2ABA (Fig. 1).

Characterization of complexes

All complexes are found to be air and light stable, non-hygroscopic, amorphous powder. The complexes are coloured and sparingly soluble in common organic solvents but appreciably soluble

in more polar aprotic solvents such as dimethyl sulphoxide and dimethyl formamide. The elemental analysis, molar conductance and magnetic moment data of the complexes of the ligand (3FI2ABA) are presented in Table 1. The analytical data of the

Table 1: Elemental analysis, molar conductance and magnetic moment studies on Mn(II), Ni(II), Cu(II) complexes of 3FI2ABA

Complex	% C	% H	% N	% Metal	Colour	M.P. (°C)	Molar conductance (ohm ⁻¹ cm ² mol ⁻¹)	Magnetic moment (μ _{eff} BM)
[MnL(Ac)(H ₂ O) ₃]	49.2 (50.1)	5.01 (4.60)	6.58 (6.50)	13.01 (12.76)	Brown	309	29	6.79
[NiLAc(H ₂ O) ₃]	51.16 (49.60)	4.01 (4.60)	6.69 (6.44)	12.36 (13.56)	Ivory	342	3	4.5
[CuLAc(H ₂ O) ₃]	48.48 (49.09)	3.81 (3.11)	6.74 (6.36)	13.98 (14.54)	Green	218	21	2.06

Table 2: Characteristic infrared absorption frequencies (cm⁻¹)

Substance	γH ₂ O	γCOO (asy)	γC=N	γCOO (sym)	γC-O	In plane bending	Out of plane bending	γM-N	γM-O
LH	-	1660	1570	1535	1294	1116	900 775	-	-
[MnL(Ac)(H ₂ O) ₃]	3305	1597	1593	1450	1238	1159	862 752	524	632
[NiL(Ac)(H ₂ O) ₃]	3304	1593	1535	1454	1240	1153	869 756	528	663
[CuL(Ac)(H ₂ O) ₃]	3275	1600	1554	1456	1234	1112	871 758	513	669

*Calculated values are in parenthesis

Table 3: Electrochemical Impedance parameters of MS specimens in 1M HCl at 28°C in the absence and presence of 3FI2ABA

c (mM)	R _s (Ωcm ²)	R _{ct} (Ωcm ²)	CPE (μF cm ⁻²)	η _{EIS} %
0	5.838	47.87	78.72	
0.2	10.82	153.4	60.98	68.8
0.5	14.66	192.6	61.57	75.1
0.7	37.69	604.8	34.3	92.1
0.8	41.65	803.6	33.39	94.0

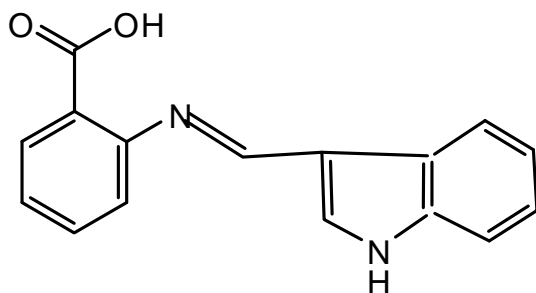


Fig. 1: Structure of the ligand (3FI2ABA)

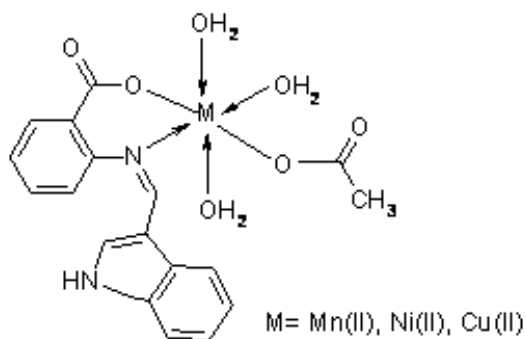


Fig. 2: Structure of complexes

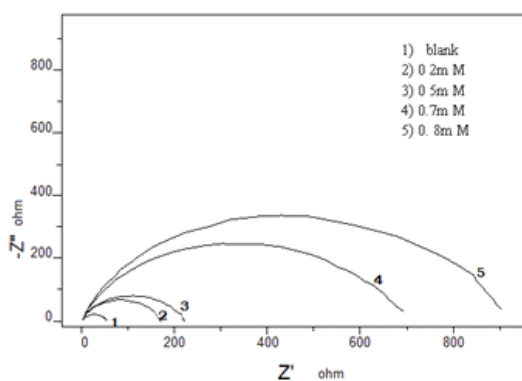


Fig. 3: Nyquist plots for MS specimens in 1M HCl in the presence and absence of the inhibitor 3FI2ABA at 28 °C

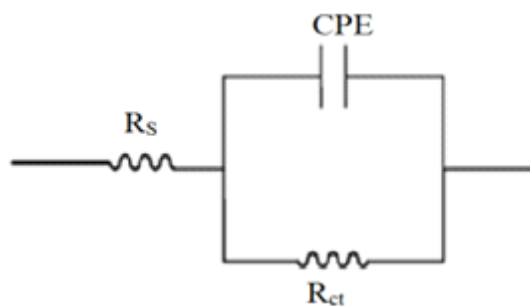


Fig. 4: Equivalent circuit fitting for EIS measurements

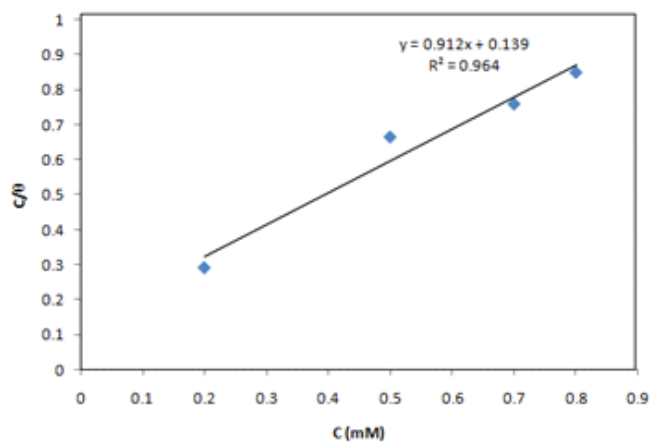


Fig. 5: Langmuir adsorption isotherm for adsorption of 3FI2ABA on MS surface in 1M HCl at 28 °C

complexes show that there is 1:1 stoichiometry between metal ion and ligand. The very low value of molar conductance data (below $30\text{ohm}^{-1}\text{cm}^2\text{mol}^{-1}$) exhibited by the complexes of the Schiff base 3FI2ABA in DMSO at a concentration of 10^{-3}molL^{-1} at $28 \pm 2^\circ\text{C}$, indicates their non-electrolytic behavior.

Magnetic moment value showed by of Mn(II) complex is 6.79BM, establishes its octahedral geometry. The Cu(II) complex exhibited slightly higher magnetic moment value (2.06BM) than expected for one unpaired electron of the d^9 electronic configuration (1.8BM). This accounts for a slight orbital contribution to the spin only value and absence of spin-spin interactions in the complex. Therefore an octahedral geometry is assigned to the copper complex. Complex of Ni(II) exhibited a slightly higher magnetic moment of 4.5BM, which may be due to the orbital contribution⁹.

Electronic spectra of Mn(II) chelate showed three weak bands at 15500, 19200 and 25600cm^{-1} which have been assigned to transition ${}^6A_{1g} \rightarrow {}^4T_{1g}(G)$, ${}^6A_{1g} \rightarrow {}^4T_{2g}(G)$ and ${}^6A_{1g} \rightarrow {}^4E_g(G)$ respectively of an octahedral field of Mn(II). The electronic spectra of Ni(II) chelate exhibited three bands with 12700, 14300 and 25100cm^{-1} which can be assigned to the transitions ${}^3A_{2g}(F) \rightarrow {}^3T_{2g}(F)$, ${}^3A_{2g}(F) \rightarrow {}^3T_{1g}(F)$ and ${}^3A_{2g}(F) \rightarrow {}^3T_{1g}(P)$ respectively. The electronic spectrum of Cu(II) contained two bands at 14100 and 15500cm^{-1} respectively. The first band can be assigned to transition ${}^2A_g \rightarrow {}^2T_g$. The second band can be attributed to the CT band.

Characteristic infrared absorption frequencies of the ligand and the complexes are represented in Table 2. Comparison of the IR spectra of the complexes with that of the ligand shows significant changes in two areas. Firstly, a band of medium intensity at about 1660cm^{-1} for the ligand, which may be attributed to the carbonyl stretching frequency of the carboxylate group, shows a shift to lower frequencies in the spectra of the complexes indicating the chelation of the ligand to metal through the carboxylate oxygen. The second region showing important changes upon ligand complexation is the $1600\text{-}1500\text{cm}^{-1}$ range. Compounds containing $>\text{C}=\text{N}-$ group have $\nu_{\text{C}=\text{N}}$ in the range $1650\text{-}1490\text{cm}^{-1}$. In this ligand, this band

occurred at 1570cm^{-1} as a strong band and has shifted to lower frequencies in the complexes indicating a reduction of electron density in the azomethine linkage at the nitrogen atom, coordinated to the metal ion⁹. In all the complexes the asymmetric and symmetric stretching vibrations of the carboxylate groups occur at $1540\text{-}1600\text{cm}^{-1}$ and $1450\text{-}1460\text{cm}^{-1}$ respectively, showing a $\Delta\nu$ of about 140cm^{-1} . Therefore monodentate nature of the carboxylate groups is indicated in the present chelates. However conclusive evidence regarding the bonding of nitrogen and oxygen are provided by the occurrence of $\nu_{\text{M-O}}$ and $\nu_{\text{M-N}}$ absorptions in the range $630\text{-}670\text{cm}^{-1}$ and $510\text{-}530\text{cm}^{-1}$ respectively in the metal complexes. The existence of a strong band at about 3300cm^{-1} in the infrared spectra of the complexes, strongly supports the presence of coordinated water molecules in these chelates.

${}^1\text{Hnmr}$ spectrum of ligand shows a characteristic peak at 12.14δ corresponding to carboxylic acid proton. In the complexes disappearance of this peak indicates the involvement of the carboxylate group in complexation by the replacement of H-atom. The azomethine proton signal undergoes a down field shift in the case of nmr spectra of the complexes. This can be attributed due to the coordination through azomethine nitrogen atom to the metal which may decrease the electron density around the $\text{CH}=\text{N}$ group proton. Significant shift in the signals at carboxylic carbon and azomethine carbon in the cmr spectrum of the complexes compared to that of ligand, establishes the involvement of these two groups in coordination. Based upon the above physico-chemical studies, octahedral geometry is suggested for Mn(II), Ni(II) and Cu(II) complexes of the ligand 3FI2ABA. Fig. 2 shows the structure of the complexes.

Electronic Impedance spectroscopy (EIS)

The corrosion response of mild steel (MS) in 1M HCl in the presence and absence of inhibitor has been investigated using Electrochemical Impedance Spectroscopy at 28°C . Fig.3 represents the Nyquist plots of MS specimens in 1M HCl. It is evident from the plots that the impedance response of metal specimens showed a marked difference in the presence and absence of the inhibitor 3FI2ABA.

The capacitance loop intersects the real axis at higher and lower frequencies. At high frequency end the intercept corresponds to the solution resistance (R_s) and at lower frequency end corresponds to the sum of R_s and charge transfer resistance (R_{ct}). The difference between the two values gives R_{ct} . The value of R_{ct} is a measure of electron transfer across the exposed area of the metal surface and it is inversely proportional to rate of corrosion¹⁰.

Impedance behaviour can be well explained by pure electric models that could verify and enable to calculate numerical values corresponding to the physical and chemical properties of electrochemical system under examination¹¹. The simple equivalent circuit that fit to many electrochemical system composed of a double layer capacitance, R_s and R_{ct} ¹²⁻¹⁴. To reduce the effects due to surface irregularities of metal, constant phase element¹⁵ (CPE) is introduced into the circuit instead of a pure double layer capacitance which gives more accurate fit as shown in the Fig.4 .

The impedance of CPE can be expressed as

$$Z_{CPE} = \frac{1}{Y_o(j\omega)^\eta} \quad \dots(2)$$

Where Y_o is the magnitude of CPE, ω is the exponent (phase shift), ω is the angular frequency and j is the imaginary unit. CPE may be resistance, capacitance and inductance depending upon the values of n ¹⁰. In all experiments the observed value of n ranges between 0.8 and 1.0, suggesting the capacitive response of CPE. The EIS parameters such as R_{ct} , R_s and CPE and the calculated values of percentage of inhibition ($\eta_{EIS\%}$) of MS specimens are listed in Table 3.

From Table 3 it is clear that R_{ct} values are increased with increasing inhibitor concentration. Decrease in capacitance values CPE with inhibitor concentration can be attributed to the decrease in local dielectric constant and /or increase in the thickness of the electrical double layer. This emphasis the action of inhibitor molecules by adsorption at the metal–solution interface¹⁴. The

percentage of inhibition ($\eta_{EIS\%}$) showed a regular increase with increase in inhibitor concentration. A maximum of 94% inhibition efficiency could be achieved at an inhibitor concentration of 0.8mM.

Adsorption isotherm and free energy of adsorption

The mechanism of adsorption and the surface behavior of organic molecules can be easily viewed through adsorption isotherms. Different models of adsorption isotherms considered are Langmiur, Temkin, Frumkin and Freundlich isotherms. For the evaluation of thermodynamic parameters it is necessary to determine the best fit isotherm with the aid of correlation coefficient (R^2). Among the isotherms mentioned above, the best description of the adsorption behavior of 3FI2ABA on MS specimens and Copper specimens in 1M HCl was Langmiur adsorption isotherm which can be expressed as

$$\frac{C}{\theta} = \frac{1}{K_{ads}} + C \quad \dots(3)$$

where C is the concentration of the inhibitor, θ is the fractional surface coverage and K_{ads} is the adsorption equilibrium constant¹⁶. Fig .5 represents the adsorption plots of 3FI2ABA obtained by EIS measurements on MS steel specimens 1M HCl at 28 °C.

From the adsorption isotherm, $K_{ads} = 7194$ and it is related to the standard free energy of adsorption ΔG_{ads}^0 , by

$$\Delta G_{ads}^0 = -RT \ln(55.5 K_{ads}) \quad \dots (4)$$

Where 55.5 is the molar concentration of water, R is the universal gas constant and T is the temperature in Kelvin¹⁶. ΔG_{ads}^0 for 3FI2ABA on MS showed negative value indicating the spontaneity of the process. The value of ΔG_{ads}^0 upto -20kJ mol^{-1} is an indication of the electrostatic interaction of the charged molecule and the charged surface of the metal (physisorption) while ΔG_{ads}^0 is more negative than -40kJ implies that inhibitor molecules are adsorbed strongly on the metal surface through co-ordinate type bond(chemisorptions)¹⁸⁻²⁰. In the present investigation, 3FI2ABA molecules showed

ΔG_{ads}^0 -32.3 kJ suggesting that the adsorption of inhibitor involves both electrostatic adsorption and chemisorption.

CONCLUSIONS

1. A novel heterocyclic Schiff base 3FI2ABA was synthesized and its chelating ability was exploited by preparing Mn(II), Ni(II) and Cu(II) complexes .
2. The Schiff base and the complexes were characterized by various analytical techniques.

3. 3FI2ABA is a good inhibitor for MS in 1M HCl. A maximum of 94% of inhibition efficiency could be achieved with this inhibitor by EIS studies.
4. The inhibition mechanism is explained by adsorption. Adsorption of Schiff base on MS obey Langmuir isotherm.
5. The thermodynamic parameters of the adsorption are calculated from the adsorption isotherm which revealed that both physisorption and chemisorption are involved in the inhibition process.

REFERENCES

1. Douglas X.West, *Coord. Chem Rev.*, **123**: 49 (1993).
2. Pandhye S. and Koffman G. B., *Coord. Chem. Rev.*, **63**: 127 (1985).
3. M.H. Salunke, Z.A. Filmwala, A.D. Kamble. *Orient. J. Chem.* **27**(3): 1243 (2011).
4. Al-Moghini. *Orient. J. Chem.* **26**(3): 753-761 (2010).
5. Joby Thomas K., and Geetha Parameswaran, *Asian. J. Chem.*, **14**: 1370 (2002).
6. Stanly Jacob K., and Geetha Parameswaran, *Corro. Sci.*, **52**: 24 (2010).
7. Raman A., *Reviews on Corrosion Inhibitor Science and Technology* vol 1. NACE, Houston, TX, 452 (1986).
8. Figgis B.N., *Introduction to Ligand Field*, Wiley Eastern Ltd., New Delhi, P.279 (1978).
9. Nakamoto K., *Infrared and Raman Spectra of Inorganic and Coordination Compounds*, 3rd Edn., John Wiley, New York, 235 (1978).
10. Rosenfield I.L., *Corrosion Inhibitors*, McGraw-Hill, New York, 387 (1981).
11. Priya A.S., Muralidharam V.S., Subramannia A., *Corrosion*, **64**: 541 (2008).
12. Ashish Kumar Singh, Sudhish Kumar Shukla, Manjeet Singh, Quraishi M.A., *Mater. Chem. Phys.*, **129**: 68 (2011).
13. El Azhar M., Mernari B., Traisnel M., Bentiss F., Lagrenée M., *Corros. Sci.*, **43**: 2229 (2001).
14. Yurt A., Balaban A., Ustün Kandemir S., Bereket G., Erk B., *Mater. Chem. Phys.*, **85**: 420 (2004).
15. Macdonald J.R., Johnson W.B., Macdonald J.R., *Theory in impedance Spectroscopy*, John Wiley & Sons, New York (1987).
16. Ma Cafferty M., Hackerman N., *J. Electrochem. Soc.*, **119**: 146 (1972).
17. Xianghong Li, Shuduan Deng, Hui Fu, Taohong Li, *Electrochim. Acta*, **54**: 4089 (2009).
18. Cano E., Polo J.L., La Iglesia A., and Bastidas J.M., *Adsorption*, **10**: 219 (2004).
19. Bentiss F., Lebrini M., Lagrenée M., *Corros. Sci.*, **47**: 2915 (2005).
20. Wei-hua Li, Qiao He, Sheng-tao Zhang, Chang-ling Pei and Bao-rong Hou *J. Appl. Electrochem.*, **38**: 289 (2008).